

1
2
3
4
5
6
7
8
9
10
11
12
13
14
15
16
17
18
19
20
21
22
23
24
25
26
27
28
29
30
31
32
33
34
35
36
37
38
39
40
41
42
43
44
45
46
47
48
49
50
51
52
53
54
55
56

Supplemental Material

SARS-CoV-2 mRNA vaccinations fail to elicit humoral and cellular immune responses in multiple sclerosis patients receiving fingolimod

Lil Meyer-Arndt^{1, 2, 3}, Julian Braun^{1, 4, *}, Florent Fauchere^{1, 4, *}, Kanika Vanshylla^{5, *}, Lucie Loyal^{1, 4}, Larissa Henze^{1, 4}, Beate Kruse^{1, 4}, Manuela Dingeldey^{1, 4}, Karsten Jürchott^{1, 4}, Maïke Mangold¹, Ardit Maraj¹, Andre Braginets¹, Chotima Böttcher⁶, Andreas Nitsche⁷, Kathrin de la Rosa⁸, Christoph Ratswohl⁸, Birgit Sawitzki⁹, Pavlo Holenya¹⁰, Ulf Reimer¹⁰, Leif E. Sander¹¹, Florian Klein^{5, 12, 13}, Friedemann Paul^{2, 14, *}, Judith Bellmann-Strobl^{2, 14, *}, Andreas Thiel^{1, 4, *§}, Claudia Giesecke-Thiel^{16, *, §}

¹ Charité - Universitätsmedizin Berlin, corporate member of Freie Universität Berlin, Humboldt-Universität zu Berlin, and Berlin Institute of Health, Regenerative Immunology and Aging, BIH Center for Regenerative Therapies, 13353 Berlin, Germany

² Charité – Universitätsmedizin Berlin, corporate member of Freie Universität Berlin, Humboldt-Universität zu Berlin, and Berlin Institute of Health, NeuroCure Clinical Research Center, 10117 Berlin, Germany

³ Charité – Universitätsmedizin Berlin, corporate member of Freie Universität Berlin, Humboldt-Universität zu Berlin, and Berlin Institute of Health, Department of Neurology with Experimental Neurology, 10117 Berlin, Germany

⁴ Si-M / “Der Simulierte Mensch” a science framework of Technische Universität Berlin and Charité - Universitätsmedizin Berlin, 10117 Berlin, Germany

⁵ Institute of Virology, Faculty of Medicine and University Hospital Cologne, University of Cologne, 50931 Cologne, Germany

⁶ Charité – Universitätsmedizin Berlin, corporate member of Freie Universität Berlin, Humboldt-Universität zu Berlin, and Berlin Institute of Health, Department of Neuropsychiatry and Laboratory of Molecular Psychiatry, 10117 Berlin, Germany

⁷ Robert Koch Institute, 13353 Berlin, Germany

⁸ Department of Cancer and Immunology, Max-Delbrück-Center for Molecular Medicine in the Helmholtz Association (MDC), 13125 Berlin, Germany

⁹ Charité - Universitätsmedizin Berlin, corporate member of Freie Universität Berlin, Humboldt-Universität zu Berlin, and Berlin Institute of Health, Institute for Medical Immunology, 13353 Berlin, Germany

¹⁰ JPT Peptide Technologies, 12489 Berlin, Germany

¹¹ Charité – Universitätsmedizin Berlin, corporate member of Freie Universität Berlin, Humboldt-Universität zu Berlin, and Berlin Institute of Health, Department of Infectious Diseases and Respiratory Medicine, 13353 Berlin, Germany

¹² German Center for Infection Research, Partner Site Bonn-Cologne, 50931 Cologne, Germany

¹³ Center for Molecular Medicine Cologne (CMMC), University of Cologne, 50931 Cologne, Germany

¹⁴ Charité – Universitätsmedizin Berlin, corporate member of Freie Universität Berlin, Humboldt-Universität zu Berlin, and Berlin Institute of Health, Experimental and Clinical Research Center, 13125 Berlin, Germany

¹⁵ Max-Delbrück-Center for Molecular Medicine in the Helmholtz Association (MDC), 13125 Berlin, Germany

¹⁶ Max Planck Institute for Molecular Genetics, 14195 Berlin, Germany

* equal contribution

§Co-Corresponding authors:

Claudia Giesecke-Thiel. Address: Max Planck Institute for Molecular Genetics, Ihnestraße 63, 14195 Berlin, Germany. Phone: 030-8413-1544. Email address: giesecke@molgen.mpg.de.

Andreas Thiel. Address: Charité - Universitätsmedizin Berlin, BIH Center for Regenerative Therapies, 13353 Berlin, Germany. Phone: 030-450-539555. Email address: andreas.thiel@charite.de.

57
58
59

Supplemental Methods

60 SARS-CoV-2 pseudovirus neutralization assay

61 SARS-CoV-2 pseudoviruses were generated by co-transfection of plasmids encoding HIV Tat, HIV Gag/Pol, HIV
62 Rev, luciferase followed by an IRES and ZsGreen, and the SARS-CoV-2 spike protein (Wu01 spike, EPI_ISL_406716)
63 into HEK 293T cells using FuGENE 6 Transfection Reagent (Promega). Virus culture supernatant was harvested at
64 48 h and 72 h post transfection and stored at -80°C till use. Harvested virus was titrated by infecting 293T
65 expressing ACE2⁴² and after a 48-hour incubation at 37°C and 5% CO₂, luciferase activity was determined after
66 addition of luciferin/lysis buffer (10 mM MgCl₂, 0.3 mM ATP, 0.5 mM Coenzyme A, 17 mM IGEPAL (all Sigma-
67 Aldrich), and 1 mM D-Luciferin (GoldBio) in Tris-HCL) using the Tristar microplate reader (Berthold).
68 Neutralization assays were performed as described before. Briefly, 3-fold serial dilutions of serum (1:10 starting
69 dilution) were co-incubated with pseudovirus supernatants for 1 h at 37°C, following which 293T-ACE-2 cells
70 were added. After 48 h at 37°C and 5% CO₂, luciferase activity was determined using the luciferin/lysis buffer.
71 Background relative light units (RLUs) of non-infected cells was subtracted and 50% inhibitory dilution (ID₅₀) were
72 calculated as the serum dilution resulting in a 50% reduction in RLU compared to the untreated virus control
73 wells. ID₅₀ values were calculated by plotting a non-linear fit dose response curve in GraphPad Prism 7.0.

74

75 SARS-CoV-2 spike epitope-specific peptide microarray

76 Peptides were synthesized and immobilized on peptide microarray slides as described previously. In brief, the
77 peptides were synthesized using SPOT synthesis, cleaved from the solid support and chemoselectively
78 immobilized on functionalized glass slides. Each peptide was deposited on the microarray in triplicates. The
79 peptide microarrays were incubated with human sera (applied dilution 1:200) in a 96-well microarray incubation
80 chamber for one hour at 30°C, followed by incubation with 0.1 µg/mL fluorescently labelled anti human IgG
81 detection antibody (Jackson ImmunoResearch). Washing steps were performed after each incubation step with
82 0.1 % Tween-20 in 1x TBS. After the final incubation step the microarrays were washed and dried. Each
83 microarray slide was scanned using a GenePix Scanner 4300 SL50 (Molecular Devices). Signal intensities were
84 evaluated using GenePix Pro 7.0 analysis software (Molecular Devices). For each peptide, the MMC2 value of the
85 three triplicates was calculated. The MMC2 value was equal to the mean value of all three instances on the
86 microarray except when the coefficient of variation (CV) – standard-deviation divided by the mean value – was
87 larger than 0.5. In this case the mean of the two values closest to each other (MC2) was assigned to MMC2.
88 Further data analysis and generation of the heatmaps was performed using the statistical computing and
89 graphics software R (Version 4.1.1, www.r-project.org).

90

91 Ex vivo T cell stimulations

92 In short, PBMC were stimulated with PepMix™ SARS-CoV-2 spike glycoprotein pool 1 (JPT) covering the N-
93 terminal aa residues 1-643 (abbreviated to "S-I") and with PepMix™ SARS-CoV-2 spike glycoprotein pool 2
94 covering the C-terminal part (aa residues 633-1273, abbreviated to "S-II") at a final concentration of 1 µg/ml per
95 peptide, respectively. Stimulation controls were performed with equal concentrations of DMSO in PBS
96 (unstimulated control) and 1 µg/ml per peptide of CEFX Ultra SuperStim pool (JPT) as positive control. All
97 approaches contained 1 µg/ml purified anti-CD28 (clone CD28.2; BD Biosciences). Incubation was performed at
98 37°C, 5% CO₂ for 16 h in the presence of 10 µg/ml brefeldin A (Sigma-Aldrich) during the last 14h. T cell
99 stimulations were stopped by incubation in 20mM EDTA for 5 min.

100

101 B cell and T cell flow cytometry

102 For S-I- and S-II-specific T cell analysis, antibodies were used as described before: CD3-FITC (REA613, Miltenyi),
103 CD4-VioGreen (REA623, Miltenyi), CD8-VioBlue (REA734, Miltenyi), CD38-APC (REA671, Miltenyi), HLA-DR-
104 PerCpVio700 (REA805, Miltenyi). For B cell status analysis: CD8 Vioblue (REA734, Miltenyi), IgD BV510 (IA6-2,
105 Biolegend), CD14 BV570 (M5E2, Biolegend), CD21 BV605 (1048, BD), CD3 FITC (REA613, Miltenyi), SLAMF7 PE
106 (162.1, Biolegend), CD27 PE-Dazzle594 (O323, Biolegend), HLADR Percp-Vio770 (REA780, Miltenyi), CD20 PE-

107 Vio770 (REA780, Miltenyi), CD38 APC (REA572, Miltenyi), CD4 AlexaFluor700 (RPA-T4, Biolegend) and CD19 APC-
108 Vio770 (REA675, Miltenyi). For intracellular staining of stimulated T cells, fixation and permeabilization were
109 performed with eBioscience™ FoxP3 fixation and PermBuffer (Invitrogen) according to the manufacturer's
110 protocol. Intracellular staining was carried out for 30 min in the dark at room temperature with 4-1BB-PE
111 (REA765, Miltenyi) and CD40L-PeVio770 (REA238, Miltenyi).

112 Peripheral blood B and T cell subsets were quantified using the following staining: 50µl of blood were stained for
113 20 minutes at room temperature in the presence of 1mg/ml Beriglobin (CSL Behring) and the following antibodies
114 at their determined optimum titration: CD4-VioBlue (REA623, Miltenyi), CD3-VioGreen (REA641, Miltenyi), HLA-
115 A2-FITC (REA517, Miltenyi), CCR7-PE (REA108, Miltenyi), CD8-PerCP (REA734, Miltenyi), CD31-PE-Vio770
116 (REA730, Miltenyi), CD19-APC (REA675, Miltenyi), CD16-AF700 (REA423, Miltenyi), CD45RA-APC-Vio770
117 (REA1047, Miltenyi). 500µl of cold Erythrocyte lysis buffer (Buffer EL, Quiagen) were added and incubated 30
118 minutes on ice. 400µl of cold PBS, BSA, 2mM EDTA were then added.

119

120

121

122

123

124

125

126

127

128

129

130

131

132

133

134

135

136

137

138

139

140

141

142

143

144

145

146

147

148

149

150

151

152

153

154

155

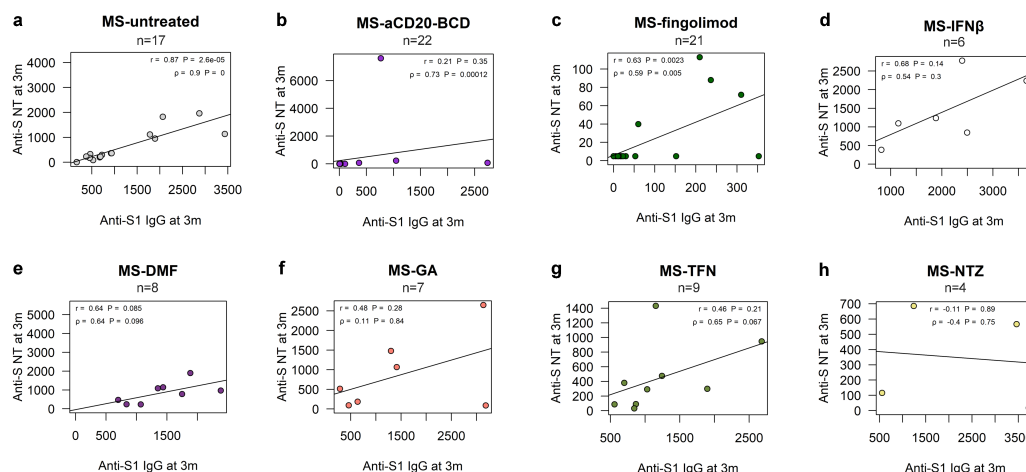
156

157
158
159

Supplemental Results

Supplemental Fig. 1

Supplemental Fig. 1

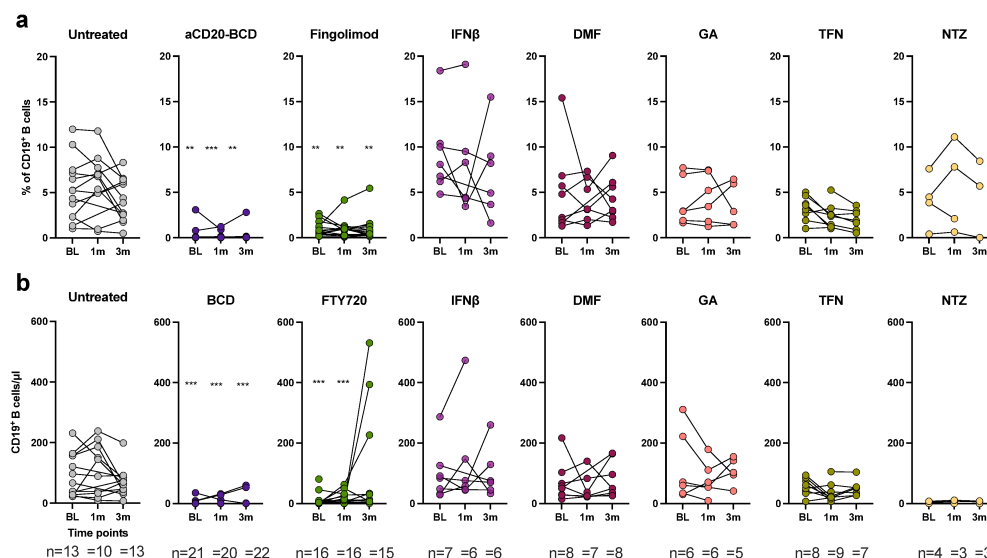


160
161
162
163
164
165
166
167
168
169

Supplemental Fig. 1. Association of anti-S1 IgG levels and neutralizing capacity. Correlation of anti-S1 IgG and neutralizing capacity in serum at 3m for untreated MS patients (MS-untreated) (a), MS-aCD20-BCD (b), and MS-FTY720 (c), MS-IFNβ (d), MS-DMF (e), MS-GA (f), MS-TFN (g), and MS-NTZ (h). Simple linear regression tests performed per treatment; correlation coefficients depicted as lines and reported as r (for Pearson correlation) and rho (for Spearman rank correlation), respectively, with corresponding p-values: Spearman r value of 0.87 for untreated MS patients, 0.68 for IFNβ, 0.64 for DMF, 0.48 for GA, 0.46 for TFN, -0.11 for NTZ, 0.2 for aCD20-BCD, and 0.64 for fingolimod.

Supplemental Fig. 2

Supplemental Fig. 2

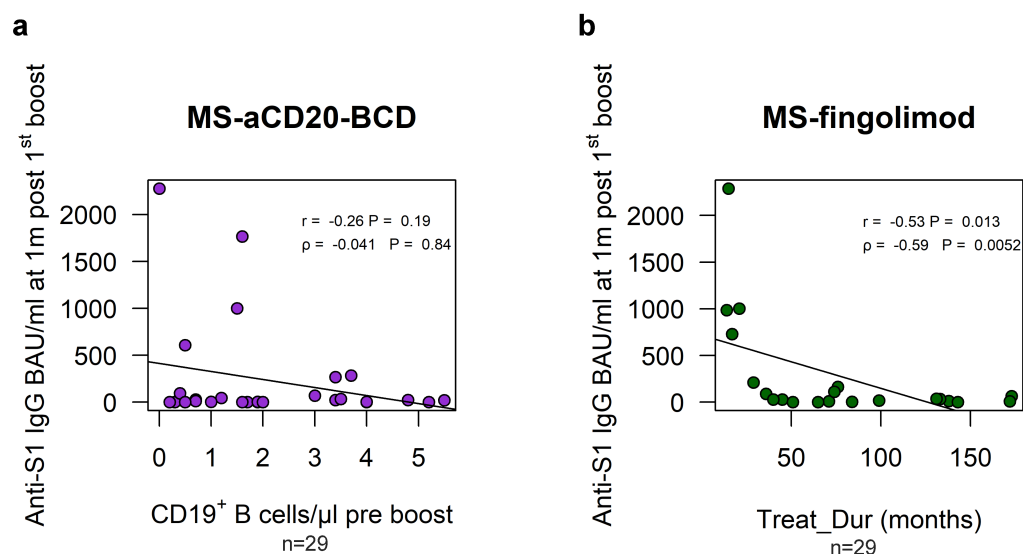


170
171
172
173
174
175

Supplemental Fig. 2. Total number and relative frequencies of peripheral blood CD19+ B cells. a) Frequencies of CD19+ B cells in total lymphocytes and b) total number of CD19+ B cells per μl per treatment group. Kruskal-Wallis test followed by Dunn's multiple comparisons test performed to test between treatment groups at the respective time point were reported for comparison to untreated patients as: *p ≤ 0.05, **p ≤ 0.01, ***p ≤ 0.001, ****p ≤ 0.0001.

176

Supplemental Fig. 3



177

178

179

180

181

182

183

184

185

186

187

188

189

190

191

192

193

194

195

196

197

198

199

200

201

202

203

204

205

206

207

208

209

210

211

212

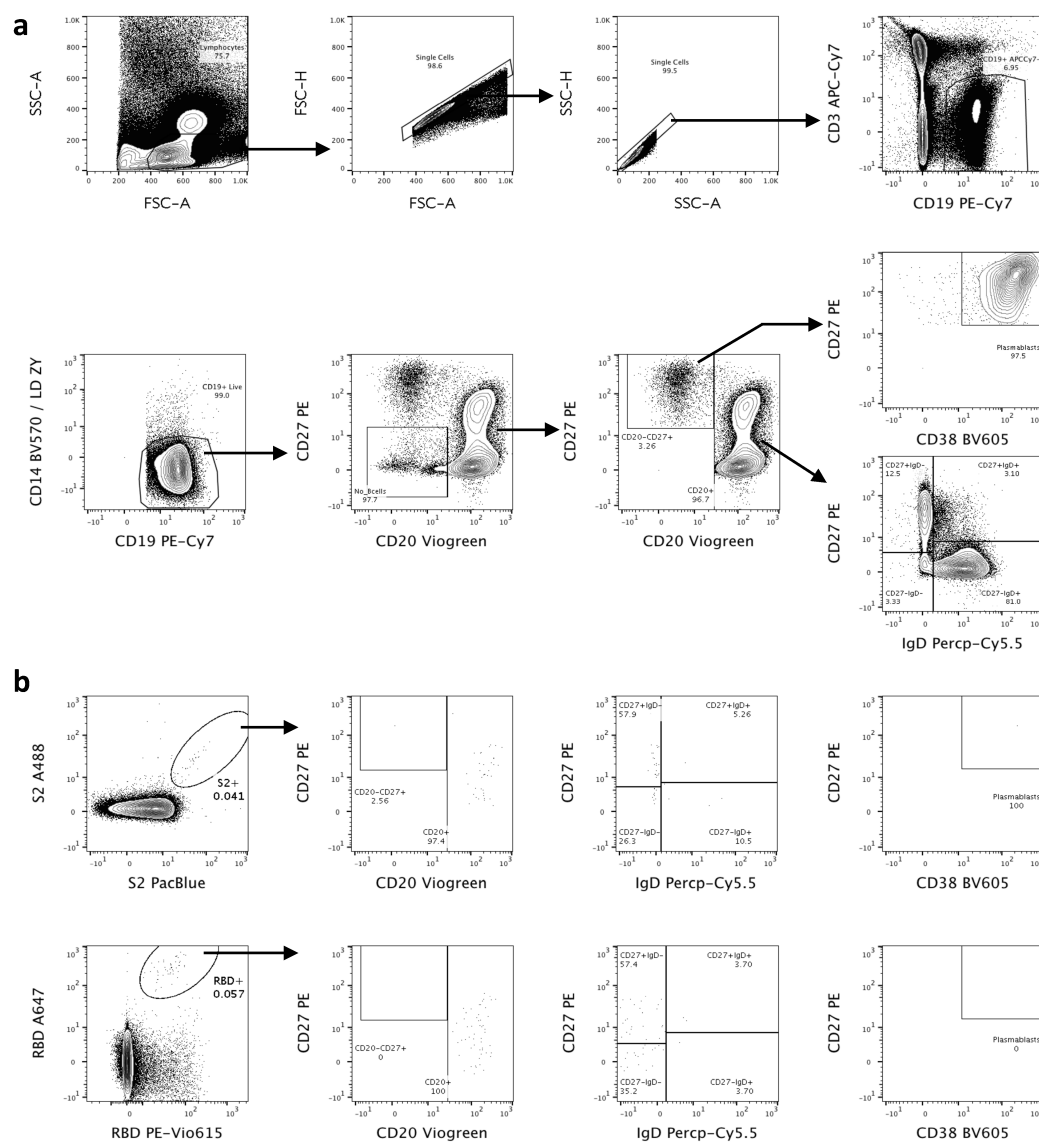
213

214

Supplemental Fig. 3. Associations of anti-S1 IgG levels 1m post 1st boost for aCD20-BCD and fingolimod. Correlation of anti-S1 IgG at 1m post 1st boost with CD19⁺ B cells/μl pre boost (aCD20-BCD; **a**) and fingolimod treatment duration in months (**b**) respectively. Simple linear regression tests performed per treatment; correlation coefficients depicted as lines and reported as r (for Pearson correlation) and ρ (for Spearman rank correlation), respectively, with corresponding p -values.

215

Supplemental Fig. 4

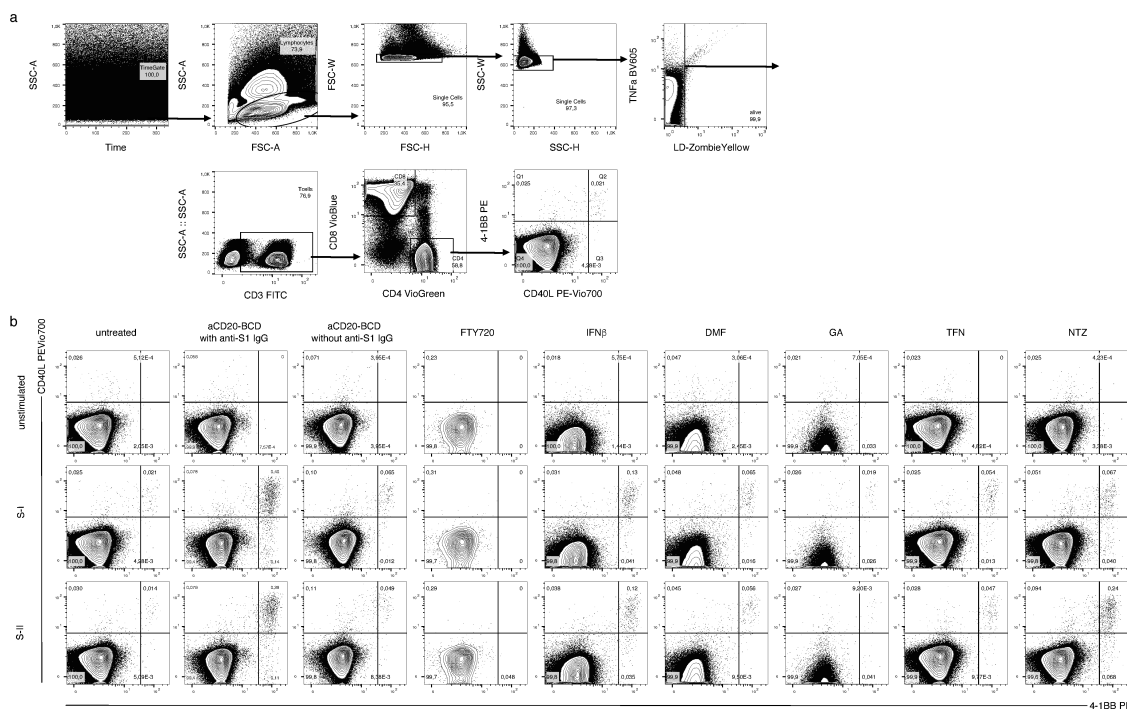


216
217
218
219
220
221
222
223
224
225
226
227
228
229
230
231
232

Supplemental Fig. 4. Gating strategy of RBD- and S2-specific B cells. **a**, B cells are gated from peripheral blood mononuclear cells (PBMCs; FSC-A vs SSC-A), by first excluding doublets (FSC-A vs FSC-H and SSC-A vs SSC-H), gating on CD19⁺CD3⁻ B cells, excluding both dead cells (LiveDead Zombie Yellow) and CD14⁺ cells, and finally by excluding CD20⁻CD27⁻ cells. Among CD19⁺CD3⁻ B cells, plasmablasts were identified as CD20^{-/low}CD27⁺⁺CD38⁺⁺ cells. CD20⁺ B cells were further classified into subpopulations based on their CD27 and IgD expression. CD20⁺CD27⁻IgD⁻ were classified as classical memory B cells (mBC), CD20⁺CD27⁺IgD⁺ were classified as double positive mBC (dp mBC), CD20⁺CD27⁻IgD⁻ were classified as double negative mBC (dn mBC), and CD20⁺CD27⁻IgD⁺ were classified as naïve B cells (nB). **b**, exemplary contour plots showing gating of S2-specific B cells and RBD-specific B cells, and again their subsequent subpopulation classification based on their CD27 and IgD expression.

233
234
235
236
237
238
239
240
241
242
243
244
245
246
247
248
249
250
251
252
253
254
255
256
257
258
259
260
261
262
263
264
265
266
267
268
269
270

Supplemental Fig. 5



Supplemental Fig. 5. Gating strategy of antigen-reactive CD4⁺ T cells and differences between DMT treatment groups. a, antigen-reactive CD40L⁺4-1BB⁺CD4⁺ T cells were gated by controlling for measurement-dependent artefacts (Time vs SSC-a) from antigen-stimulated PBMC (FSC-A vs SSC-A), by first excluding doublets (FSC-H vs FSC-W and SSC-H vs SSC-W), dead cells (LiveDead Zombie Yellow), then gating on CD3⁺ T cells and CD4⁺ double positive cells. b, exemplary contour plots showing CD40L and 4-1BB expression in unstimulated control, S-I-, and S-II-stimulated CD4⁺ T cells, displayed for the seven different DMT treatment groups at around two months after secondary SARS-CoV-2 mRNA vaccination.

Supplemental Table 1

aCD20-BCD treatment	Days since last treatment before 1 st vaccination	CD19 ⁺ B cells per μl before 1 st vaccination	Days since last treatment before booster	CD19 ⁺ B cells per μl before booster
Ocrelizumab	68	0	65	0.5
Ocrelizumab	133	0	87	0.3
Ocrelizumab	91	0.1	125	1.9
Ocrelizumab	93	0.3	143	5.5
Ocrelizumab	64	0	105	1.7
Ocrelizumab	154	35		
Ocrelizumab	162	9.2	96	3.7
Ocrelizumab	56	0.1	100	1.2
Ocrelizumab	269	8.2		
Ocrelizumab	114	0.1	360	3.4
Ocrelizumab	114	0	102	1
Ocrelizumab	144	0	116	4.8
Ocrelizumab	45	0.2	58	1.9
Ocrelizumab	114	2.5		
Ocrelizumab	94	0	84	5.2

Ocrelizumab	92	0.1		
Ocrelizumab	130	0	82	4
Ocrelizumab	97	0.7	120	0.7
Rituximab	103	0.1		
Rituximab	120	0.1	103	3.5
Rituximab	101	2.3	111	1.5
Ocrelizumab	112		179	1.6
Ocrelizumab	104			
Ocrelizumab	117		149	3.4
Ocrelizumab	92		105	0.2
Ocrelizumab	77		99	0.7
Ocrelizumab	94		314	378.1
Ocrelizumab			83	4
Ocrelizumab			99	0.2
Ocrelizumab			129	0
Ocrelizumab			45	1.5
Ocrelizumab			68	2
Ocrelizumab			92	0.5
Ocrelizumab			93	3
Ocrelizumab				
Ocrelizumab			94	1.6

271
272
273
274
275
276
277
278
279
280
281
282

Supplemental Table 1. Days since last aCD20-BCD treatment administration and absolute B cell numbers before primary and booster vaccinations. 22 patients treated with aCD20-BCD therapies were enrolled prior to primary vaccination, another 5 after secondary vaccination (before 3m) and another 9 before booster vaccinations who received either rituximab or ocrelizumab (dosage per administration: 1000 mg rituximab or 600 mg ocrelizumab) in 6-month intervals (except for one patient whose next treatment interval was delayed due to low lymphocyte counts).